ChemPubSoc Europe

DOI: 10.1002/cmdc.201200411

Small-Molecule APOBEC3G DNA Cytosine Deaminase Inhibitors Based on a 4-Amino-1,2,4-triazole-3-thiol Scaffold

Margaret E. Olson,[a] Ming Li,[b] Reuben S. Harris,[b] and Daniel A. Harki*[a]

APOBEC3G (A3G) is a single-stranded DNA cytosine deaminase that functions in innate immunity against retroviruses and retrotransposons. Although A3G can potently restrict Vif-deficient HIV-1 replication by catalyzing excessive levels of G→A hypermutation, sublethal levels of A3G-catalyzed mutation may contribute to the high level of HIV-1 fitness and its incurable prognosis. To chemically modulate A3G catalytic activity with the goal of decreasing the HIV-1 genomic mutation rate, we synthesized and biochemically evaluated a class of 4-amino-1,2,4-triazole-3-thiol small-molecule inhibitors identified by high-throughput screening. This class of compounds exhibits low-micromolar (3.9–8.2 μM) inhibitory potency and remarkable specificity for A3G versus the related cytosine deaminase, APOBEC3A. Chemical modification of inhibitors, A3G mutational screening, and thiol reactivity studies implicate C321, a residue proximal to the active site, as the critical A3G target for this class of molecules.

Introduction

Since the discovery of acquired immune deficiency syndrome (AIDS) and the identification of human immunodeficiency virus (HIV), the causative retrovirus of AIDS, a wealth of biochemical and immunological investigation has fueled the development of more than 25 antiretrovirals and the introduction of highly active antiretroviral therapy (HAART).[1,2] Although these therapies have slowed the global AIDS epidemic and drastically prolonged the life expectancy of HIV-1-positive patients, the imminent development of drug resistance and the toxic side effects associated with HAART prompt continued efforts toward the discovery of new therapeutics with unique mechanisms of action.[3]

Research over the past decade has elucidated a previously unknown mechanism of host–virus interaction between a family of retrovirus restriction factors found in human host cells, namely APOBEC3D, APOBEC3F, APOBEC3G, and APOBEC3H, and the virally encoded virion infectivity factor (Vif).[4–6] APOBEC3G (apolipoprotein B mRNA editing enzyme, catalytic polypeptide-like 3G; A3G), a single-stranded (ss)DNA cytosine-to-uracil (C→U) deaminase and the archetypal member of this family, is a potent restrictor of Vif-deficient HIV-1 replication. Wild-type virus, however, uses Vif to nucleate the formation of an E3 ubiquitin ligase complex that degrades A3G and enables virus replication in A3G-expressing cells. The APOBEC3–Vif interaction is therefore essential for HIV-1 infection and provides a novel and minimally explored target in HIV-1 drug discovery.

Current models hypothesize that A3G restricts HIV-1 replication by incorporating into budding viral particles by an RNA–Gag interaction, hijacking transport with the particle until a target cell is infected, and inhibiting viral cDNA synthesis via both deamination-independent[7] and deamination-dependent mechanisms.[4,5,8–10] Deamination-independent inhibition of HIV-1 replication is predicted to occur through direct A3G interaction with viral genomic RNA, causing physical blockage to HIV-1 reverse transcriptase progression. The prominent mechanism by which A3G restricts Vif-deficient HIV-1 replication, however, is through C→U deamination events on minus-strand viral DNA that become immortalized as G→A hypermutations in the plus (genomic) strand. Such extensive mutation ultimately renders the virus non-infective.

The potent anti-HIV-1 activity of A3G has recently sparked efforts to discover inhibitors of Vif, agonists of A3G, and molecules that mask the A3G–Vif interaction surface.[11–17] Small molecules that antagonize Vif reinstate the innate antiviral activity of A3G by boosting G→A hypermutation, accomplishing lethal mutagenesis. Inhibitor design strategies to increase the HIV-1 mutation rate can be defined as *therapy by hypermutation*.[18]

Conversely, there is strong evidence to support the hypothesis that HIV-1 exploits A3G through modulation by Vif. By taking advantage of the pro-mutational capacities of A3G, HIV-1 can accomplish an advantageous level of sublethal mutation to enable viral fitness.[18–21] Sequenced genomes from HIV-1-positive patients support this model by exhibiting considerable A3G-dependent mutation patterns despite the ability of Vif to trigger A3G degradation.[22,23] Thus, genetic variation attributable to A3G likely contributes to the characteristically high mu-

[a] *M. E. Olson, Prof. Dr. D. A. Harki*
Department of Medicinal Chemistry, University of Minnesota – Twin Cities
717 Delaware Street S.E., Minneapolis, MN 55414 (USA)
E-mail: daharki@umn.edu

[b] *Dr. M. Li, Dr. R. S. Harris*
Department of Biochemistry, Molecular Biology & Biophysics
University of Minnesota – Twin Cities
321 Church Street, Minneapolis, MN 55455 (USA)

Supporting information for this article is available on the WWW under http://dx.doi.org/10.1002/cmdc.201200411.

tation rate of HIV-1, its ability to evade immune clearance mechanisms, and its rapid evolution of resistance to antiretroviral therapies. Therefore, A3G-catalyzed mutation may be essential for HIV-1 to achieve its unprecedented level of viral fitness, and current therapies and vaccination strategies may benefit from dampening A3G activity, as HIV-1 evolution would be predicted to slow. Our strategy to decrease the HIV-1 mutation rate by inhibiting A3G can be classified as *therapy by hypomutation*.[18]

We recently described the development of a fluorescence-based high-throughput screening (HTS) assay that was used to identify small-molecule inhibitors of A3G.[24] In our previous study, screening of 1280 pharmacologically active compounds (LOPAC, Sigma) demonstrated the A3G-specific inhibitory capacities of catechol-containing scaffolds, including our prototype A3G antagonist MN30 ($IC_{50}=9.1\ \mu M$, PubChem CID-5353329). Mutational screening, structural analysis, and mass spectrometry identified C321, located proximal to the active site, as the binding site for these catechol-based A3G inhibitors. To identify additional A3G-specific inhibitors with unique chemotypes, we screened over 325 000 compounds (Sanford–Burnham Medical Research Institute, NIH MLPCN collection) using our fluorescence-based A3A/A3G DNA cytosine deamination assay.[25] A class of 4-amino-1,2,4-triazole-3-thiols and structurally related analogues were identified and developed as A3G inhibitors based on MLS-0036803, a HTS hit renamed MN256.0105 (**1**) in-house (Figure 1). Scaffolds identical or analogous to **1** have been previously investigated for fungicidal,[26] antioxidant,[27] cytotoxic,[28] antimicrobial,[28] and anti-osteoarthritic[29] applications.

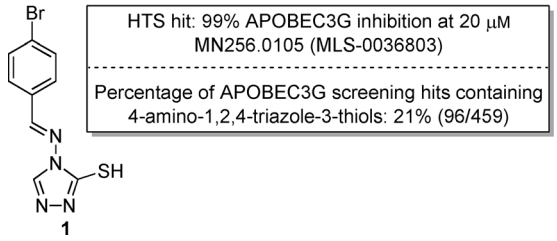

Figure 1. Structure of A3G inhibitor MN256.0105 (**1**) and the frequency at which the 4-amino-1,2,4-triazole-3-thiol substructure was observed in A3G hits from high-throughput screening.

Results and Discussion

Synthesis of 4-amino-1,2,4-triazole-3-thiol analogues

To elucidate the mechanism of inhibition for the 4-amino-1,2,4-triazole-3-thiol class of screening hits and to reconfirm the original lead molecule, MN256.0105 (**1**) was synthesized (Scheme 1). 4-Amino-1,2,4-triazole-3-thiol (**4**) was obtained in high yield by reaction of thiocarbohydrazide (**2**) in aqueous formic acid at reflux. Recrystallization from ethanol yielded pure **4** in 95% yield. Compound **1** was then obtained in 82% yield by condensation of **4** with *para*-bromobenzaldehyde in excess acetic acid. Analogue **8** was similarly synthesized in two steps, first by reaction of thiocarbohydrazide with acetic acid

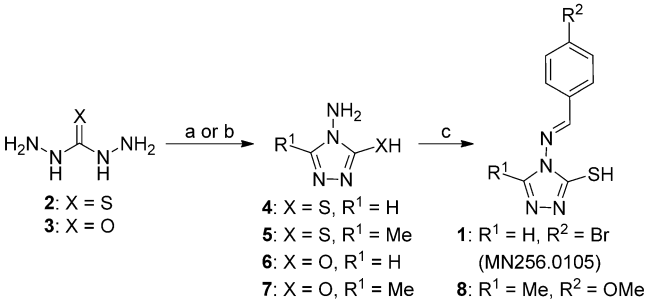

Scheme 1. *Reagents and conditions:* a) $HCO_2H_{(aq)}$ or AcOH, reflux (to dryness), 95%–quant. (for **4** and **5**); b) $(EtO)_3CH$ or $(EtO)_3CCH_3$, 60 °C–reflux, 34–69% (for **6** and **7**); c) *p*-BrC_6H_4CHO or *p*-$MeOC_6H_4CHO$, AcOH, reflux, 82–84%.

at reflux to yield heterocycle **5**. The highest yields were accomplished by introducing an empty Dean–Stark trap to remove excess acetic acid by distillation upon conclusion of the reaction, as opposed to the previously reported method of concentration in vacuo.[30] Imine formation by reaction with *para*-anisaldehyde under acidic conditions delivered **8** (83%, two steps).

Chemical modification of the 4-amino-1,2,4-triazole-3-thiol heterocycle **4** was pursued to evaluate the necessity of the thiol. As shown in Scheme 1, the thiol moiety of congeners **4** and **5** was replaced by a hydroxy group to deliver **6** and **7**. These scaffolds were prepared by treating carbohydrazide (**3**) with excess triethylorthoformate (for **6**) or triethylorthoacetate (for **7**) to achieve the core 4-amino-1,2,4-triazole-3-ol heterocycles in 69 and 34% yields, respectively.

We were also interested in evaluating scaffolds similar to **1** that were not subject to imine hydrolysis to evaluate the effects of the additional aromatic functionality on A3G inhibitory potency. The synthesis of non-hydrolysable amide **9** was accomplished in moderate yield through treatment of amine **5** with benzoyl chloride in dioxane at reflux (Scheme 2). We additionally pursued thiol protection methodologies to further gauge the necessity of a free sulfhydryl group for biological potency. For this investigation, we synthesized conjugated thiadiazole **10** and S-alkylated benzyl analogue **11**. Compound **10** was prepared by treatment of **5** with *para*-methoxybenzonitrile and aqueous phosphoric acid at elevated temperatures (47% yield). Benzyl protection of **5** was carried out by reaction

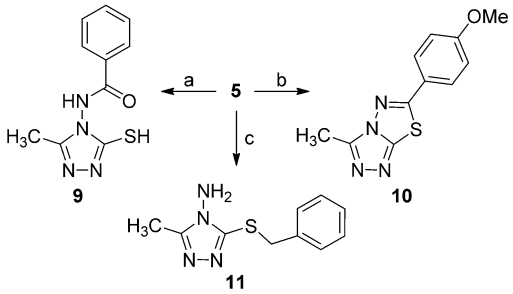

Scheme 2. *Reagents and conditions:* a) BzCl, dioxane, reflux, 44%; b) *p*-$MeOC_6H_4CN$, $H_3PO_{4(aq)}$, reflux, 47%; c) BnBr, NaH, DMF, RT, 14%.

with benzyl bromide, in yields consistent with previous reports, to afford compound **11**.[31]

Biological evaluation of synthetic analogues

Synthesized small molecules were evaluated for A3G inhibition with our fluorescence-based deamination assay.[24] Using full-length human A3G purified from HEK293T cells and an ssDNA oligonucleotide functionalized with a 5′-6-FAM fluorophore and a 3′-TAMRA quenching molecule, deamination efficiency was quantified by measured fluorescence. In the absence of inhibitor, deamination of the target cytosine to uracil (C→U) is followed by uracil DNA glycosylase catalyzed excision of U and sodium hydroxide catalyzed phosphodiester backbone cleavage, which releases the 6-FAM fluorophore from the TAMRA quench. Dose–response curves were generated to determine IC_{50} values for synthesized analogues (Table 1).

Table 1. APOBEC3G inhibition by compounds **1** and **4**–**11**.

Candidate Inhibitor	IC_{50} [μM][a]
1	4.3 ± 1.1
4	No Activity
5	6.1 ± 1.1
6	No Activity
7	No Activity
8	3.9 ± 1.2
9	8.2 ± 1.2
10	No Activity
11	No Activity

[a] Assays performed in triplicate; values are the mean ± SD.

Synthesized **1** exhibited A3G inhibitory activity equivalent to that of the HTS material, verifying results obtained from preliminary A3G inhibition (IC_{50} = 4.3 ± 1.1 μM versus IC_{50} = 2.0 μM, respectively). Structurally related analogue **8** (IC_{50} = 3.9 ± 1.2 μM) demonstrated equipotent anti-A3G activity to HTS hit **1** (Table 1). As a result, we hypothesized that small modifications to the phenyl and triazole rings have little effect on A3G inhibition.

Based on previous work with MN30,[24] we hypothesized that the thiol functionalities of **1** and **8** garnered the A3G inhibitory activity. Moreover, the suspected hydrolytic susceptibility of Schiff bases **1** and **8** under biological conditions prompted us to test the 4-amino-1,2,4-triazole-3-thiol precursors **4** and **5** as A3G inhibitors. Surprisingly, **4** did not display any inhibitory activity at 100 μM, whereas the related 5-methyl analogue **5** (IC_{50} = 6.1 ± 1.1 μM) was found to be nearly equipotent to its parent scaffold **8** (IC_{50} = 3.9 ± 1.2 μM). Incorporation of a non-hydrolysable linker, yielding **9**, maintained inhibition (IC_{50} = 8.2 ± 1.2 μM), demonstrating that pendent aromatic functionalities on the exocyclic amine have little effect on the potency of A3G inhibition by molecules of this class.

To demonstrate the necessity of the thiol component of these scaffolds, hydroxy-substituted analogues **6** and **7** were tested against purified A3G. No inhibitory activity was detected for either molecule (Table 1). Furthermore, evaluation of thiol-alkylated scaffolds **10** and **11** revealed no A3G inhibition, further demonstrating the necessity of the free thiol.

In addition to screening against wild-type A3G, compounds **1** and **4**–**11** were tested for inhibitory activity against the related cytosine deaminase, APOBEC3A (A3A), to gauge inhibitor specificity. The primary structure of A3A is 65% identical and 73% similar to the A3G C-terminal catalytic domain. Remarkably, analogues **1** and **4**–**11** all failed to inhibit A3A activity at doses up to 100 μM, despite the inherent reactivity of the thiol functionality. To begin querying if molecules of this class can exhibit activity in cells, we screened **1** and **4**–**11** for inhibitory activity against A3G in HEK293T cell lysates. Unfortunately, no measureable amounts of A3G inhibition were detected for any of the molecules screened. Consequently, the reactive thiol moiety may be unavailable for A3G inhibition in the complex environment of cell lysates.

Reactivity studies of APOBEC3G inhibitors with cysteine-like substrates

The known reactivity properties of thiols with cysteine residues prompted our evaluation of this scaffold to form disulfide bonds under biological conditions. Amide analogue **9**, which contains a free thiol, was dissolved in DMSO, diluted with PBS buffer (pH 7.4) and treated with excess cysteamine. Reaction aliquots were removed at the following time points: 0 min, 30 min, 1 h, and 12 h, and were analyzed by reversed-phase (RP)-HPLC for the presence of new peaks. Complete disappearance of the starting material was observed within 30 min yielding one new product, which was characterized as disulfide **12** by mass spectrometry (Figure 2). Therefore, molecules of this class that contain free thiols are capable of intercepting other thiols and forming disulfide bonds, which may confer their primary mechanism of enzyme inhibition.

Mutation studies identify C321 as the inhibitor binding site

Because free thiols are required for A3G inhibition by molecules of this class, the surface cysteine residues of A3G were investigated as potential inhibitor binding sites. Previous work has demonstrated that cysteine 321 (C321) of the catalytic A3G domain is an inhibitor binding site for covalent modification by small molecules.[24] Employing this methodology, a triple mutant construct A3G 2K3A, which has three surface Cys→Ala substitutions (namely C243A, C321A, and C356A), and a single mutant A3G C321A were tested in parallel with wild-type enzyme against thiols **1** and **8** using the previously described deamination assay.[24] Importantly, in the context of full-length A3G, these specific substitutions have no effect on localization, deamination, oligomerization, or HIV-1 Vif-deficient restriction capabilities.[24,32,33]

We found that the mutant enzymes were only partially resistant to compounds **1** and **8**, with recovered deamination efficiency between 19–46% (Figure 3). Interestingly, deaminase activity was not fully recovered relative to DMSO control or the previously reported catechol-based covalent inhibitor MN30.[24]

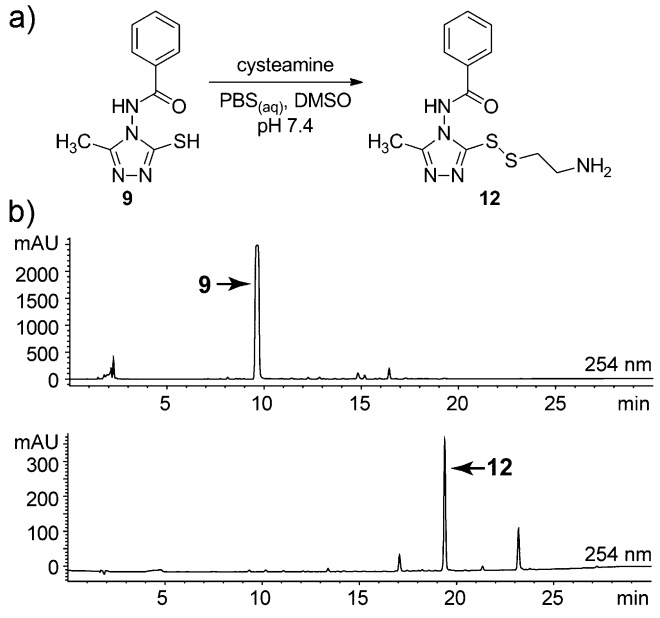

Figure 2. a) 4-Amino-1,2,4-triazole-3-thiol (**9**) and cysteamine were shaken in aqueous PBS (pH 7.4) at 37 °C. Aliquots were analyzed by RP-HPLC at $t=0$, 30, 60 min, and 12 h. b) Reaction at $t=0$ min (top) and $t=12$ h (bottom); peak **12** was isolated and characterized by HRMS-ESI$^+$ m/z $[M+Na]^+$ calcd: 332.0616, found: 332.0629.

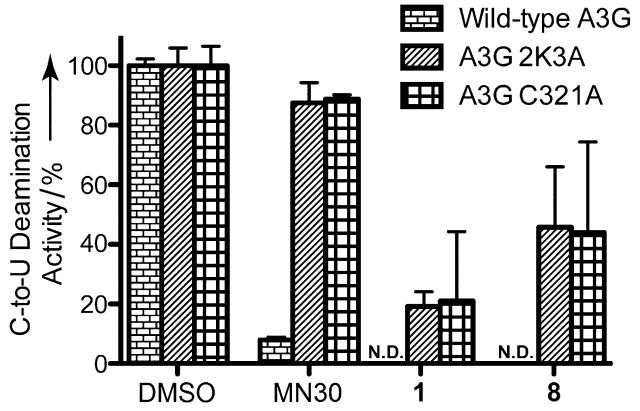

Figure 3. Potency of MN30 (Supporting Information figure S1), **1**, and **8** against wild-type A3G and mutants A3G 2K3A and A3G C321A. The mean and SD of triplicate deaminase assays with 50 μM compound are shown relative to control (DMSO only); N.D.: not detectable.

Such results imply that these thiol-containing inhibitors may also function, at least in part, through a second inhibitory mechanism. Initial hypotheses derived from the field of transition-metal catalysis suggest that the 4-amino-1,2,4-triazole-3-thiol scaffold chelates divalent metals.[34–37] A3G, which contains a catalytic zinc atom, may therefore suffer a decrease in deaminase efficiency in the presence of zinc-chelating molecules; however, additional experiments are necessary to validate this possibility.

Conclusions

High-throughput screening and analogue synthesis have identified a class of 4-amino-1,2,4-triazole-3-thiols that inhibit the DNA cytosine deaminase A3G. Counter-screening of the small-molecule analogues against related APOBEC3 family member A3A demonstrated marked specificity for A3G inhibition despite the reactivity of the inhibitors to sulfur nucleophiles. Replacement or protection of thiol moieties completely abrogated their inhibitory capabilities, providing evidence that a free thiol is a key structural feature of this class of inhibitors. A combination of mutagenesis studies and HPLC assays indicate that the inhibitory activity of this class of molecules is accomplished through disulfide bond formation with C321, a residue adjacent to the A3G active site. These findings further support our hypothesis that covalent modification to C321 causes conformational change to the A3G protein, where Y315 shifts and sterically blocks substrate DNA cytosine residues from entering the A3G active site.[24]

Mutant screening potentially implicates a second mechanism of action based on the inability of the C321A mutant to fully recover deamination capabilities in comparison with DMSO control. We hypothesize that the 4-amino-1,2,4-triazole-3-thiol scaffold may engage the catalytic zinc atom in A3G, conferring a secondary mechanism of enzyme inhibition, although more evidence is needed to support this theory.

Experimental Section

General synthesis

Reagents were purchased from Sigma–Aldrich, Alfa Aesar, or Acros and were used without additional purification. Bulk solvents were obtained from Fisher Scientific, and anhydrous solvents were purchased from Sigma–Aldrich. Reactions were performed under an atmosphere of dry N_2 unless otherwise noted. Silica gel chromatography was performed on a Teledyne-Isco Combiflash R_f-200 instrument using Redisep R_f Gold High-Performance silica gel columns (Teledyne-Isco) or self-packed columns with SiliaFlash 60 Å silica gel (SiliCycle). HPLC analyses were performed on an Agilent 1200 series instrument equipped with a diode array detector and a Zorbax SB-C_{18} column (4.6×150 mm, 3.5 μm, Agilent Technologies) or a Zorbax SB-AQ column (4.6×150 mm, 3.5 μm, Agilent Technologies) for analytical-scale analysis. Compounds used in biological testing were ≥98% pure, as determined by two-wavelength HPLC analysis (λ 254 and 215 nm), except for compounds **4** and **8**, which were 92 and 93% pure, respectively. NMR spectroscopy was performed with a Bruker Avance instrument operating at 400 MHz (for ^{1}H) and 100 MHz (for ^{13}C) at ambient temperature. Chemical shifts are reported in parts per million and are normalized to internal solvent peaks or $(CH_3)_4Si$ ($\delta=0$ ppm). Exchangeable protons (thiols, alcohols, and amines) were verified by ^{1}H NMR D_2O exchange experiments. High-resolution mass spectrometry (HRMS) data were collected in positive-ion mode on a Bruker BioTOF II instrument.

4-Amino-1,2,4-triazole-3-thiol (4): Prepared as previously described.[38] ^{1}H NMR ([D_6]DMSO): $\delta=13.63$ (s, 1H, SH), 8.45 (s, 1H), 5.68 ppm (s, 2H, NH_2); ^{13}C NMR ([D_6]DMSO): $\delta=166.0$, 142.3 ppm; HRMS-ESI$^+$ m/z $[M+Na]^+$ calcd for $C_2H_4N_4S$: 139.0054, found: 139.0045.

4-[(4-Bromobenzylidene)amino]-1,2,4-triazole-3-thiol (1): *p*-Bromobenzaldehyde (0.349 g, 1.89 mmol) was added to a solution of 4-amino-1,2,4-triazole-3-thiol (**4**, 0.219 g, 1.89 mmol) in AcOH (8.0 mL) at room temperature. The reaction was then heated at reflux. After 2 h, the reaction was cooled and poured into ice water. The resulting precipitate was collected, washed with H_2O, and recrystallized from hot, absolute EtOH to yield compound **1** as a pale-yellow solid (0.438 g, 82%): ^{1}H NMR ($CDCl_3$): $\delta = 10.47$ (s, 1H), 8.08 (s, 1H), 7.73 (d, $J = 2.0$ Hz, 2H), 7.63 ppm (d, $J = 2.0$ Hz, 2H); ^{13}C NMR ($CDCl_3$): $\delta = 158.83$, 158.78, 140.9, 132.4, 131.2, 130.0, 127.3 ppm; HRMS-ESI$^+$ *m/z* $[M+Na]^+$ calcd for $C_9H_7BrN_4S$: 304.9472, found: 304.9468.

4-Amino-5-methyl-1,2,4-triazole-3-thiol (5): A mixture of thiocarbohydrazide (**2**, 2.60 g, 24.5 mmol) in AcOH (5.0 mL) in a 100-mL round-bottom flask was heated at reflux into an empty Dean–Stark trap. Because product formation is kinetically rapid, this process served to remove excess acid which enhanced reaction yields. The reaction was allowed to proceed until product formed as a white precipitate and all acid was removed. The residual solid was removed from the flask with H_2O, filtered, and recrystallized from hot, aqueous EtOH to yield compound **5** as a white powder (3.16 g, 99%): ^{1}H NMR ([D$_6$]DMSO): $\delta = 13.39$ (s, 1H, SH), 5.51 (s, 2H, NH_2), 2.11 ppm (s, 3H, CH_3); ^{13}C NMR ([D$_6$]DMSO): $\delta = 165.37$, 149.08, 10.37 ppm; HRMS-ESI$^+$ *m/z* $[M+Na]^+$ calcd for $C_3H_6N_4S$: 153.0211, found: 153.0213.

4-Amino-1,2,4-triazol-3-ol (6): Prepared as previously described.[39] ^{1}H NMR ([D$_6$]DMSO): $\delta = 11.52$ (s, 1H, OH), 7.80 (s, 1H), 5.26 ppm (2H, NH_2); ^{13}C NMR ([D$_6$]DMSO): $\delta = 154.2$, 139.3 ppm; HRMS-ESI$^+$ *m/z* $[M+Na]^+$ calcd for $C_2H_4N_4O$: 123.0283, found: 123.0292.

4-Amino-5-methyl-1,2,4-triazol-3-ol (7): Carbohydrazide (**3**, 0.500 g, 5.550 mmol) was suspended in triethylorthoacetate (1 mL), heated from 60 to 90 °C over 45 min, and then held at reflux. After 2 h, the reaction was cooled, concentrated in vacuo, and the crude solid was recrystallized from hot, absolute EtOH to yield compound **7** as a white crystalline solid (0.214 g, 34%): ^{1}H NMR ([D$_6$]DMSO): $\delta = 11.23$ (s, 1H, OH), 5.10 (s, 2H, NH_2), 2.07 ppm (s, 3H); ^{13}C NMR ([D$_6$]DMSO): $\delta = 154.3$, 145.4, 10.7 ppm; HRMS-ESI$^+$ *m/z* $[M+H]^+$ calcd for $C_3H_6N_4O$: 115.0614, found: 115.0615.

4-[(4-Methoxybenzylidene)amino]-5-methyl-1,2,4-triazole-3-thiol (8): *p*-Anisaldehyde (93 μL, 0.800 mmol) was added to a solution of **3** (0.100 g, 0.768 mmol) in AcOH (3.5 mL) at room temperature. The reaction was heated at reflux for 2 h, then cooled and poured into ice water. The resulting precipitate was collected and washed with H_2O to yield compound **8** as a pale-yellow solid (0.160 g, 84%) without further purification: ^{1}H NMR ([D$_6$]DMSO): $\delta = 13.67$ (s, 1H), 9.71 (s, 1H), 7.86 (d, $J = 8.0$ Hz, 2H), 7.10 (d, $J = 8.0$ Hz, 2H), 3.85 (s, 3H), 2.32 ppm (s, 3H); ^{13}C NMR ($CDCl_3$): $\delta = 163.3$, 162.4, 161.5, 149.8, 130.8, 125.2, 114.6, 55.6, 11.3 ppm; HRMS-ESI$^+$ *m/z* $[M+Na]^+$ calcd for $C_{11}H_{12}N_4OS$: 271.0630, found: 271.0617.

***N*-(3-Thio-5-methyl-1,2,4-triazol-4-yl)benzamide (9)**: A solution of **3** (0.100 g, 0.770 mmol) in dioxane (5 mL) was treated with benzoyl chloride (100 μL, 0.770 mmol) and heated at reflux for 24 h. The reaction mixture was cooled to room temperature and concentrated in vacuo. SiO_2 purification (gradient 40→100% EtOAc in hexanes) gave compound **9** as a white solid (80.0 mg, 44%): ^{1}H NMR ([D$_6$]DMSO): $\delta = 13.73$ (s, 1H, SH), 11.78 (s, 1H, NH), 8.01–7.98 (m, 2H), 7.71–7.57 (m, 3H), 2.20 ppm (s, 3H); ^{13}C NMR ([D$_6$]DMSO): $\delta =$ 167.0, 165.4, 149.9, 132.9, 130.9, 128.8, 127.9, 10.0 ppm; HRMS-ESI$^+$ *m/z* $[M+Na]^+$ calcd for $C_{11}H_{11}N_3OS$: 257.0473, found: 257.0288.

6-(4-Methoxyphenyl)-3-methyl-1,2,4-triazolo[3,4-*b*]-[1,3,4]thiadiazole (10): *p*-Methoxybenzonitrile (0.100 g, 0.75 mmol) and **5** (0.098 g, 0.75 mmol) were suspended in aqueous H_3PO_4 (5 mL) and heated at reflux. After 5 h, the mixture was diluted with excess H_2O, neutralized with aqueous NaOH (40% *w/v*) to pH 7–8, and concentrated in vacuo to yield compound **10** as a pale-yellow powder (0.087 g, 47%): ^{1}H NMR ($CDCl_3$): $\delta = 7.83$ (d, $J = 8.0$ Hz, 2H), 7.03 (d, $J = 8.0$ Hz, 2H), 3.90 (s, 3H), 2.76 ppm (s, 3H); ^{13}C NMR ($CDCl_3$): $\delta = 166.2$, 163.2, 153.1, 144.9, 129.0, 122.1, 115.0, 55.8, 10.6 ppm; HRMS-ESI$^+$ *m/z* $[M+Na]^+$ calcd for $C_{12}H_{11}N_3OS$: 269.0473, found: 269.0468.

3-(Benzylthio)-5-methyl-1,2,4-triazol-4-amine (11): Prepared as previously described.[31] ^{1}H NMR ($CDCl_3$): $\delta = 7.45$–7.43 (m, 2H), 7.36–7.30 (m, 3H), 4.60 (s, 2H), 2.37 ppm (s, 3H); ^{13}C NMR ([D$_6$]DMSO): $\delta = 158.7$, 152.0, 137.1, 128.7, 127.7, 127.1, 34.4, 10.8 ppm; HRMS-ESI$^+$ *m/z* $[M+H]^+$ calcd for $C_{10}H_{12}N_4S$: 221.0861, found: 221.0871.

Biological assays

Expression and purification of APOBEC3A, APOBEC3G, APOBEC3G 2K3A and APOBEC3G C321A: A3G, A3A, A3G 2K3A and A3G C321A were expressed and purified as previously described.[24]

DNA deaminase assays: The DNA deaminase assay was performed as previously described with the ssDNA oligomer 5′-(6-FAM)-AAA-TAT-TCC-CTA-ATA-GAT-AAT-GTG-A-(TAMRA)-3′.[24] Deaminase assays with mutant A3G were performed with 50 μM compound, 0.0675 μM A3G, 0.33 μM ssDNA, and excess uracil DNA glycosylase (UDG). None of the synthesized compounds inhibited UDG in the context of the in vitro assay.

HPLC assays for disulfide formation: A solution of **9** (10.0 mg, 0.040 mmol) in DMSO (100 μL) was diluted with 1× aqueous PBS (5 mL, pH 7.4) and treated with cysteamine (0.684 g, 4.03 mmol, 100 equiv). The solution was then shaken at 37 °C. Aliquots of the reaction mixture were taken at the following time points: 0 min, 30 min, 60 min, and 12 h. These reaction aliquots were analyzed by analytical RP-HPLC. The HPLC analytical method (Zorbax SB-C_{18} 4.6×150 mm, 3.5 μm column, Agilent Technologies; flow rate: 1.0 mL min^{-1}) involved isocratic 10% CH_3CN in 0.1% (*v/v*) aqueous CF_3CO_2H (0–2 min), followed by linear gradients of 10→85% CH_3CN (2–24 min) and 85→95% CH_3CN (24–26 min). The major peak **12** (Figure 2) was isolated, concentrated in vacuo, and characterized by mass spectrometry; HRMS-ESI$^+$ *m/z* $[M+Na]^+$ calcd for $C_{12}H_{15}N_5OS_2$: 332.0616, found: 332.0629.

Acknowledgements

We acknowledge financial support from a University of Minnesota Innovation Grant (to D.A.H. and R.S.H.), the NIH (P01GM091743 to R.S.H.), and startup funds from the Department of Medicinal Chemistry and College of Pharmacy (to D.A.H.). M.E.O thanks the NIH for a Chemistry–Biology Interface Predoctoral Traineeship (T32-GM08700) and Dr. Lyle and Sharon Bighley and the College of Pharmacy for a Bighley Graduate Fellowship.

Keywords: antiviral agents · APOBEC3G · drug discovery · heterocycles · hypomutation

[1] Y. Mehellou, E. De Clercq, *J. Med. Chem.* **2010**, *53*, 521 – 538.
[2] M. A. Thompson, J. A. Aberg, P. Cahn, J. S. Montaner, G. Rizzardini, A. Telenti, J. M. Gatell, H. F. Gunthard, S. M. Hammer, M. S. Hirsch, D. M. Jacobsen, P. Reiss, D. D. Richman, P. A. Volberding, P. Yeni, R. T. Schooley, *JAMA J. Am. Med. Assoc.* **2010**, *304*, 321 – 333.
[3] P. A. Volberding, S. G. Deeks, *Lancet* **2010**, *376*, 49 – 62.
[4] J. S. Albin, R. S. Harris, *Expert Rev. Mol. Med.* **2010**, *12*, e4.
[5] M. H. Malim, M. Emerman, *Cell Host Microbe* **2008**, *3*, 388 – 398.
[6] J. F. Hultquist, J. A. Lengyel, E. W. Refsland, R. S. LaRue, L. Lackey, W. L. Brown, R. S. Harris, *J. Virol.* **2011**, *85*, 11220 – 11234.
[7] K. N. Bishop, M. Verma, E.-Y. Kim, S. M. Wolinsky, M. H. Malim, *PLoS Pathog.* **2008**, *4*, e1000231.
[8] A. J. Schumacher, G. Haché, D. A. Macduff, W. L. Brown, R. S. Harris, *J. Virol.* **2008**, *82*, 2652 – 2660.
[9] E. Miyagi, S. Opi, H. Takeuchi, M. Khan, R. Goila-Gaur, S. Kao, K. Strebel, *J. Virol.* **2007**, *81*, 13346 – 13353.
[10] E. P. Browne, C. Allers, N. R. Landau, *Virology* **2009**, *387*, 313 – 321.
[11] J. L. Smith, W. Bu, R. C. Burdick, V. K. Pathak, *Trends Pharmacol. Sci.* **2009**, *30*, 638 – 646.
[12] Z. Xiao, E. Ehrlich, K. Luo, Y. Xiong, X.-F. Yu, *FASEB J.* **2007**, *21*, 217 – 222.
[13] R. Nathans, H. Cao, N. Sharova, A. Ali, M. Sharkey, R. Stranska, M. Stevenson, T. M. Rana, *Nat. Biotechnol.* **2008**, *26*, 1187 – 1192.
[14] S. Cen, Z.-G. Peng, X.-Y. Li, Z.-R. Li, J. Ma, Y.-M. Wang, B. Fan, X.-F. You, Y.-P. Wang, F. Liu, R.-G. Shao, L.-X. Zhao, L. Yu, J.-D. Jiang, *J. Biol. Chem.* **2010**, *285*, 16546 – 16552.
[15] T. Ejima, M. Hirota, T. Mizukami, M. Otsuka, M. Fujita, *Int. J. Mol. Med.* **2011**, *28*, 613 – 616.
[16] A. Ali, J. Wang, R. S. Nathans, H. Cao, N. Sharova, M. Stevenson, T. M. Rana, *ChemMedChem* **2012**, *7*, 1217 – 1229.
[17] I. Mohammed, M. K. Parai, X. Jiang, N. Sharova, G. Singh, M. Stevenson, T. M. Rana, *ACS Med. Chem. Lett.* **2012**, *3*, 465 – 469.
[18] R. S. Harris, *Nat. Biotechnol.* **2008**, *26*, 1089 – 1090.
[19] G. Haché, L. M. Mansky, R. S. Harris, *AIDS Rev.* **2006**, *8*, 148 – 157.
[20] H. A. Sadler, M. D. Stenglein, R. S. Harris, L. M. Mansky, *J. Virol.* **2010**, *84*, 7396 – 7404.
[21] L. C. F. Mulder, A. Harari, V. Simon, *Proc. Natl. Acad. Sci. USA* **2008**, *105*, 5501 – 5506.
[22] C. Pace, J. Keller, D. Nolan, I. James, S. Gaudieri, C. Moore, S. Mallal, *J. Virol.* **2006**, *80*, 9259 – 9269.
[23] N. Wood, T. Bhattacharya, B. F. Keele, E. Giorgi, M. Liu, B. Gaschen, M. Daniels, G. Ferrari, B. F. Haynes, A. McMichael, G. M. Shaw, B. H. Hahn, B. Korber, C. Seoighe, *PLoS Pathog.* **2009**, *5*, e1000414.
[24] M. Li, S. M. Shandilya, M. A. Carpenter, A. Rathore, W. L. Brown, A. L. Perkins, D. A. Harki, J. Solberg, D. J. Hook, K. K. Pandey, M. A. Parniak, J. R. Johnson, N. J. Krogan, M. Somasundaran, A. Ali, C. A. Schiffer, R. S. Harris, *ACS Chem. Biol.* **2012**, *7*, 506 – 517.
[25] M. Li, R. S. Harris, unpublished results.
[26] X. Sun, Y. Tao, Y. Liu, Y. Jia, B. Chen, *Acta Chim. Sin.* **2008**, *66*, 234 – 238.
[27] A. M. Demchenko, V. O. Yanchenko, O. S. Smolskiy, V. O. Aheyev, M. O. Lozynskiy, *Farm. Zh.* **2004**, *1*, 68.
[28] S. M. Badr, R. M. Barwa, *Bioorg. Med. Chem.* **2011**, *19*, 4506 – 4512.
[29] L. Maingot, F. Leroux, V. Landry, J. Dumont, H. Nagase, B. Villoutreix, O. Sperandio, R. Deprez-Poulain, B. Deprez, *Bioorg. Med. Chem. Lett.* **2010**, *20*, 6213 – 6216.
[30] N. F. Eweiss, A. A. Bahajaj, E. A. Elsherbini, *J. Heterocycl. Chem.* **1986**, *23*, 1451 – 1458.
[31] D. D. J. Cartwright, B. A. J. Clark, H. McNab, *J. Chem. Soc. Perkin Trans. 1* **2001**, 424 – 428.
[32] E. Harjes, P. J. Gross, K.-M. Chen, Y. Lu, K. Shindo, R. Nowarski, J. D. Gross, M. Kotler, R. S. Harris, H. Matsuo, *J. Mol. Biol.* **2009**, *389*, 819 – 832.
[33] S. M. D. Shandilya, M. N. L. Nalam, E. A. Nalivaika, P. J. Gross, J. C. Valesano, K. Shindo, M. Li, M. Munson, W. E. Royer, E. Harjes, T. Kono, H. Matsuo, R. S. Harris, M. Somasundaran, C. A. Schiffer, *Structure* **2010**, *18*, 28 – 38.
[34] K. Singh, D. P. Singh, M. S. Barwa, P. Tyagi, Y. Mirza, *J. Enzyme Inhib. Med. Chem.* **2006**, *21*, 557 – 562.
[35] K. Singh, D. P. Singh, M. S. Barwa, P. Tyagi, Y. Mirza, *J. Enzyme Inhib. Med. Chem.* **2006**, *21*, 749 – 755.
[36] M. Tabatabaee, M. Ghassemzadeh, A. Sadeghi, M. Shahriary, B. Neumüller, A. Rothenberger, *Z. Anorg. Allg. Chem.* **2009**, *635*, 120 – 124.
[37] M. Ghassemzadeh, M. Tabatabaee, S. Soleimani, B. Neumüller, *Z. Anorg. Allg. Chem.* **2005**, *631*, 1871 – 1876.
[38] R. M. McCarrick, M. J. Eltzroth, P. J. Squattrito, *Inorg. Chim. Acta* **2000**, *311*, 95 – 105.
[39] J. Zhang, T. Zhang, K. Yu, *Chem. Heterocycl. Compd.* **2003**, *39*, 461 – 466.

Received: September 5, 2012
Revised: October 24, 2012
Published online on November 23, 2012